3-Hydroxyquinoxaline–2–carboxalidine–2–amino –5–methylphenol complexes of manganese(II), iron(III), cobalt(II), nickel(II), copper(II) and zinc(II)

Contents

5.1 Introduction

5.2 Experimental

5.3 Results and discussion

5.4 Conclusions

References

5.1 INTRODUCTION

The syntheses of ONO donor Schiff base complexes attract considerable attention due to its applications in catalysis, photonics and medicine [1-3]. The Schiff base derived from salicylaldehyde and 2–aminophenol is well studied [4-7]. Several metal chelates coordinated through the Schiff base ONO donors have been studied as oxygen carriers and they are useful models for bioinorganic processes [8, 9]. Patel *et al.* [10, 11] reported the crystal structures of the copper(II) complex of N-(salicylidene)anthranilic acid with imidazole, 2,2'-bipyridine or 1,10-phenanthroline as coligands. These complexes were screened for superoxide dismutase activity. The ONO donor Schiff bases derived from salicylaldehyde and their transition metal complexes can be considered as non-enzymatic models for pyridoxal amino acid systems. The chemistry of the metal complexes of ONO donor Schiff bases is quite interesting because of their biological applications [12-15].

Quinoxalines with ortho hydroxy groups are of particular interest due to their ability to form tautomers. They can form complexes in either neutral keto form or enolic form as given in Figure 5.1. Eventhough quinoxalines and their compounds have been extensively studied [16-21], the reports on the quinoxaline based Schiff bases are very scanty. The synthesis and characterization of quinoxaline-2-carboxaldehyde with 2-aminophenol was previously reported [22]. Our aim was to prepare new tridentate ONO donor Schiff base from 3-hydroxyquinoxaline-2-carboxaldehyde and 2-amino-5-methylphenol and study the nature of its complexes.
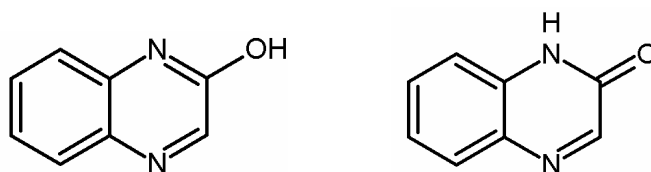

Figure 5.1: *Tautomeric forms of 2−hydroxyquinoxaline*

We have synthesized the Schiff base, 3-{(*E*)-[(2-hydroxy-4-methylphenyl) imino]methyl} quinoxalin-2(1*H*)-one, by condensation reaction. The Schiff base is an ONO donor and it can act as a monobasic or dibasic ligand due to the formation of tautomers. In solid state the keto form is predominant and it easily enolise in solution to form diol. The results of the studies on the complex formation of this ligand with Mn(II), Fe(III), Co(II), Ni(II), Cu(II) and Zn(II) ions are presented in this chapter.

5.2 EXPERIMENTAL

5.2.1 Materials and methods

The preparation of 3−hydroxyquinoxaline−2−carboxaldehyde and techniques employed for the characterization of ligand and metal complexes are given in chapter II.

5.2.2 Synthesis of 3-{(*E*)-[(2-hydroxy-4-methylphenyl) imino]methyl} quinoxalin-2(1*H*)-one (hamp)

To an aqueous solution of 3−hydroxyquinoxaline−2−carboxaldehyde (1.742 g, 10 mmol, in 500 mL distilled water), 3−4 drops of conc. HCl was added. To this solution was added dropwise 2−amino−5−methylphenol (1.231 g, 10 mmol) in methanol (20 mL). The solution was stirred for 6 hours. The red coloured Schiff base formed was filtered, washed with water and dried over anhydrous calcium chloride. The crude product was recrystallised from absolute ethanol. Formation of hamp is presented in scheme 5.1.

(Yield: 75 %, MP: 220 ºC)
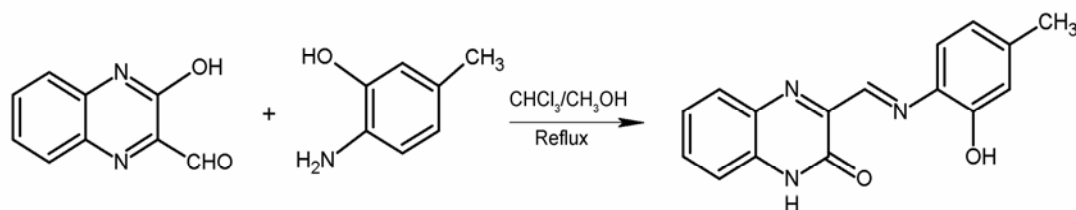
Scheme 5.1: *The formation of hamp by condensation*

5.2.3 Preparation of Complexes

The Schiff base, hamp, (0.01 mol, 0.279 g) was dissolved in 50 mL methanol. To this solution a solution of metal compound (0.01 mol: manganese acetate tetrahydrate 0.245 g, ferric chloride 0.162 g, cobalt acetate hexahydrate 0.249 g, zinc acetate 0.219 g, cupric acetate 0.198 g or nickel acetate 0.249 g) in methanol (30 mL) was added. The solution was then refluxed for an hour and was then kept at room temperature (28±2 ºC) after reducing its volume by evaporation. The precipitate formed was filtered, washed with methanol and kept in a desiccator. The formation of metal complexes is given in Scheme 5.2.
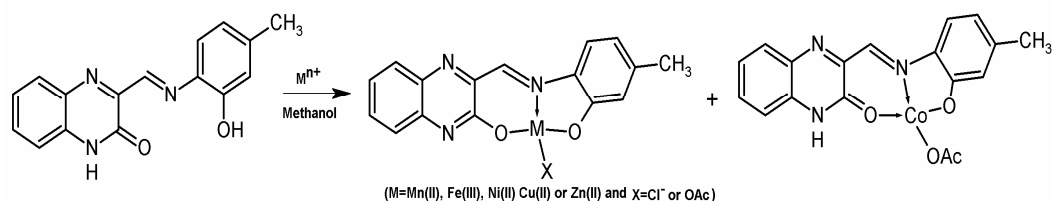
Scheme 5.2: *The formation of metal complexes of hamp*

5.3 RESULTS AND DISCUSSION

The complexes are stable in air and non-hygroscopic. They are soluble in common solvents like ethanol, methanol, acetonitrile and DMF. The analytical data (Table 5.1) reveal that all the complexes are formed in metal:ligand ratio of 1:1. Further the molecular formula of the complexes given in the table agrees well with the analytical data. The very low conductance values (Table 5.2) of the complexes in DMF indicate the non-electrolytic nature of the complexes [23].

Table 5.1: *Analytical data of qamp and its complexes*

| Compound | Colour | Yield (%) | Analytical data. Found (calculated)% | | | | |
			C	H	N	M	Cl
hamp	Red	85	69.15 (68.81)	4.55 (4.69)	14.05 (14.00)	-	-
[Mn(hamp)(H$_2$O)].H$_2$O	Brown	45	51.36 (52.19)	3.29 (4.11)	10.89 (11.41)	14.85 (14.92)	-
[Fe(hamp)Cl(H$_2$O)$_2$]	Black	58	47.43 (47.50)	3.77 (3.74)	10.45 (10.39)	13.67 (13.80)	8.69 (8.76)
[Co(hamp)(OAc)(H$_2$O)$_2$].H$_2$O	Violet	71	47.96 (48.01)	4.71 (4.70)	9.15 (9.33)	13.11 (13.09)	-
[Ni(hamp)(H$_2$O)].H$_2$O	Black	65	51.49 (51.66)	4.11 (4.06)	11.39 (11.30)	15.73 (15.78)	-
[Cu(hamp)(H$_2$O)]	Black	80	53.21 (53.55)	3.66 (3.65)	11.69 (11.71)	17.77 (17.71)	-
[Zn(hamp)(H$_2$O)]	Brown	70	53.19 (53.28)	3.67 (3.63)	11.66 (11.65)	18.17 (18.13)	-

Table 5.2: *Conductivity and magnetic moment data of complexes*

Compound	λ_m[#]	μ_{eff} (B.M)
[Mn(hamp)(H$_2$O)].H$_2$O	13	5.75
[Fe(hamp)Cl(H$_2$O)$_2$]	18	5.40
[Co(hamp)(OAc)(H$_2$O)$_2$].H$_2$O	21	4.95
[Ni(hamp)(H$_2$O)].H$_2$O	9	3.84
[Cu(hamp)(H$_2$O)]	17	2.10
[Zn(hamp)(H$_2$O)]	11	-

[#] Molar conductivity (in Mho cm^2 mol^{-1}), 10^{-3} Molar solution in DMF

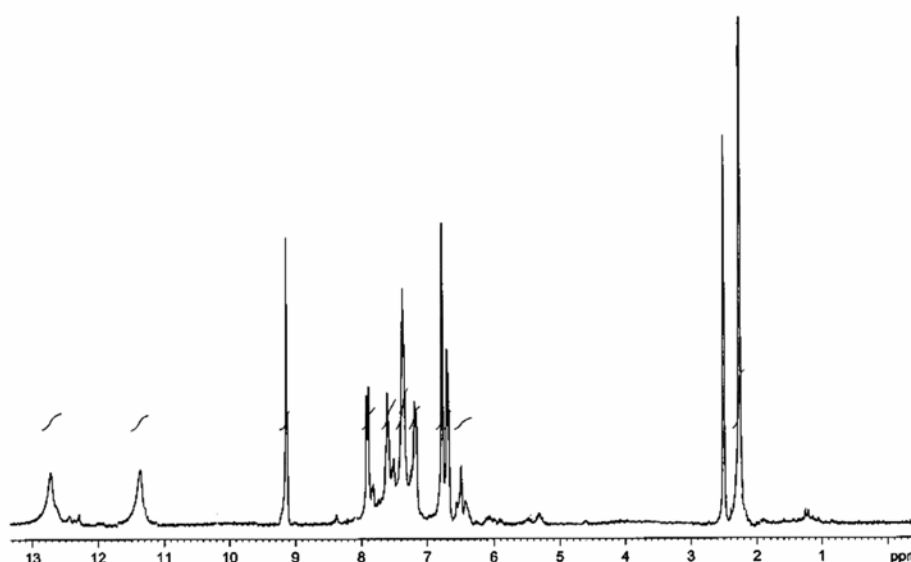## 5.3.1 ^{1}H NMR spectrum of hamp and [Zn(hamp)(H$_2$O)]

The ^{1}H NMR spectrum of hamp and that of the zinc(II) complex are given in Figures 5.2 and 5.3. The spectral data are summerised in Table 5.3. Because of the low solubility in CDCl$_3$, the NMR spectra of the Schiff base and zinc(II) complex were made in deuterated DMSO. The spectral features suggest that the compound exist as keto tautomer. The co-existence of the tautomers is not observed. The broad singlet observed at 12.85 ppm is due to phenolic –OH proton. The broadness of the band indicates considerable hydrogen bonding in the Schiff base. The peak observed at 11.52 ppm is due to NH proton [24-26]. The azomethine proton resonates at 9.15 ppm which is a singlet [27]. The multiplet observed around 6.40-8.30 ppm is due to aromatic protons of quinoxaline ring and phenolic ring. The peak due to methyl protons is observed at 2.26 ppm as a singlet.

The NMR spectrum of the zinc(II) complex is given in Figure 5.3. The phenolic OH and NH signals which are found at 12.85 and 11.52 ppm in the spectrum of the ligand are not seen in the spectrum of the Zn(II) complex indicating the enolisation of the Schiff base in zinc(II) complex and participation of the phenolic OH group in chelation with proton displacement [28, 29]. The signals due to azomethine proton are shifted upon complexation, which is probably due to

Transition metal complexes of quinoxaline based Schiff base ligands: Synthesis,
characterization and catalytic activity study

109

the donation of the lone pair of electrons by the nitrogen to the central metal atom [30]. ^{1}H NMR spectrum gives the aromatic and quinoxaline protons as a number of complex multiplets in the region δ 7.10–7.98 ppm. The methyl group attached to the phenolic ring is observed at 2.22 ppm as a singlet. The broad singlet in the region 3.51– 3.80 ppm indicates the presence of a water molecule in the complex.

Table 5.3: ^{1}H NMR Spectroscopic data of hamp

Compound	Chemical shift, δ (ppm)	Assignment
hamp	12.85	(s br, 1H, OH)
	11.52	(s, 1H, NH)
	9.15	(s, 1H, CH azomethine)
	6.40-8.30	(m, 7H, Ar H)
	2.26	(s, 3H, CH3)
[Zn(hamp)(H$_2$O)]	9.30	(s, 1H, CH azomethine)
	7.10-7.98	(m, 7H, Ar H)
	3.51-3.80	(br s, 2 H, water)
	2.22	(s, 3H, CH$_3$)

Figure 5.2: ^{1}H NMR spectrum of hamp
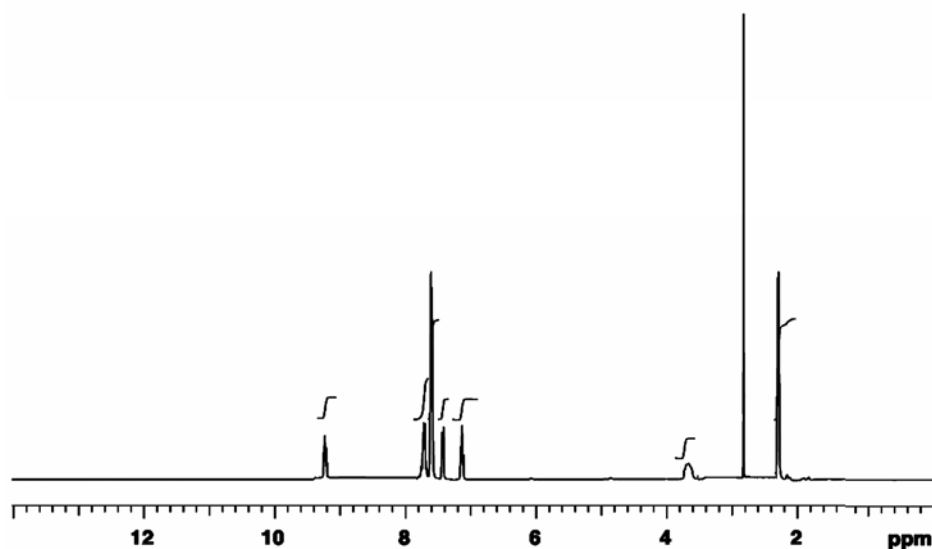
Figure 5.3: *¹H NMR spectrum of [Zn(hamp)(H₂O)]*

5.3.2 Magnetic susceptibility measurements

The magnetic moment values (at 28±2 ºC) of the complexes are shown in Table 5.2. The μ_{eff} value of the Mn(II) complex was found to be 5.75 B.M. as expected for high spin d^5 system. The iron(III) complex shows a magnetic moment of 5.80 B.M. The cobalt(II) complex has a magnetic moment of 4.95 B.M. and the high magnetic moment value is as expected for high spin Co(II) octahedral complex. The higher magnetic moment is due to the orbital contribution [31]. The nickel(II) complex exhibits a magnetic moment value of 3.84 B.M., which is in the normal range observed for tetrahedral Ni(II) complexes. The higher value of magnetic moment compared to the expected spin only value is due to the orbital contribution [32]. The magnetic moment of the copper(II) complex is 2.10 B.M. which suggest absence of Cu–Cu interactions. The higher value indicates a tetrahedral structure.

5.3.3 Infrared spectra

The infrared spectral bands and the assignments are given in Table 5.4. The IR spectra of ligand and complexes are given in Figures 5.4 to 5.10. The band at

3386 cm^{-1} in the spectrum of hamp is due to the OH stretching vibrations. The ligand exhibits azomethine C=N stretching at 1609 cm^{-1} and C=N of quinoxaline ring at 1571 cm^{-1} [33-37]. There is a sharp intense band at 1665 cm^{-1}, which shows the presence of a keto group in the compound and confirms the existence of tautomerism for the 2-hydroxyquinoxaline moiety.

Most of the bands due to the free ligand are present in the spectra of complexes. A new broad band at around 3300 cm^{-1} is seen for all the complexes which may be due to the presence of hydrated or coordinated water molecule [38]. The azomethine C=N stretching is observed at a lower frequency than that for the ligand. This negative shift in C=N stretching frequency is an indication of coordination of nitrogen [39-41]. For all the complexes the phenolic C-O stretching occurs at higher wavenumber when compared to that of the ligand indicating the deprotonation and coordination of the hydroxyl groups. In addition, the FTIR spectra of all complexes, except that of the cobalt(II) complex, do not contain $v(C=O)$, which indicates the enolisation of the keto group in solution. The strong band observed at 1633 cm^{-1} for the cobalt(II) complex suggests that the Schiff base acts as a monobasic tridentate ligand. Appearance of new bands in the spectra of all complexes in the regions 500–450 and 420–400 cm^{-1} has been attributed to $v(M-O)$ and $v(M-N)$, respectively.

Table 5.4: *IR spectral data of hamp and its complexes*

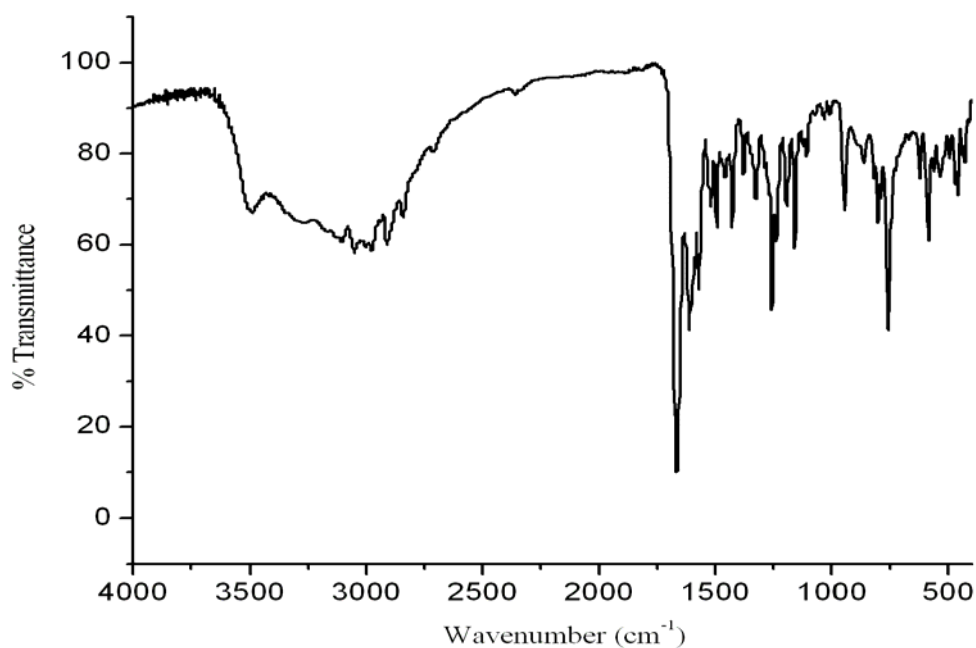| Assignments (in cm⁻¹)	v (OH)	v (C=O)	v (C=N) *	v (C–O)#	v (M–O)	v (M–N)
hamp	3386	1665	1609	1254	-	-
[Mn(hamp)(H₂O)].H₂O	3376	-	1592	1260	492	417
[Fe(hamp)Cl(H₂O)₂]	3450	-	1589	1259	490	424
[Co(hamp)(OAc)(H₂O)₂].H₂O	3390	1633	1604	1255	473	414
[Ni(hamp)(H₂O)].H₂O	3370	-	1601	1257	484	409
[Cu(hamp)(H₂O)]	3361	-	1602	1259	472	414
[Zn(hamp) (H₂O)]	3365	-	1603	1259	471	417

* azomethine, # phenolic

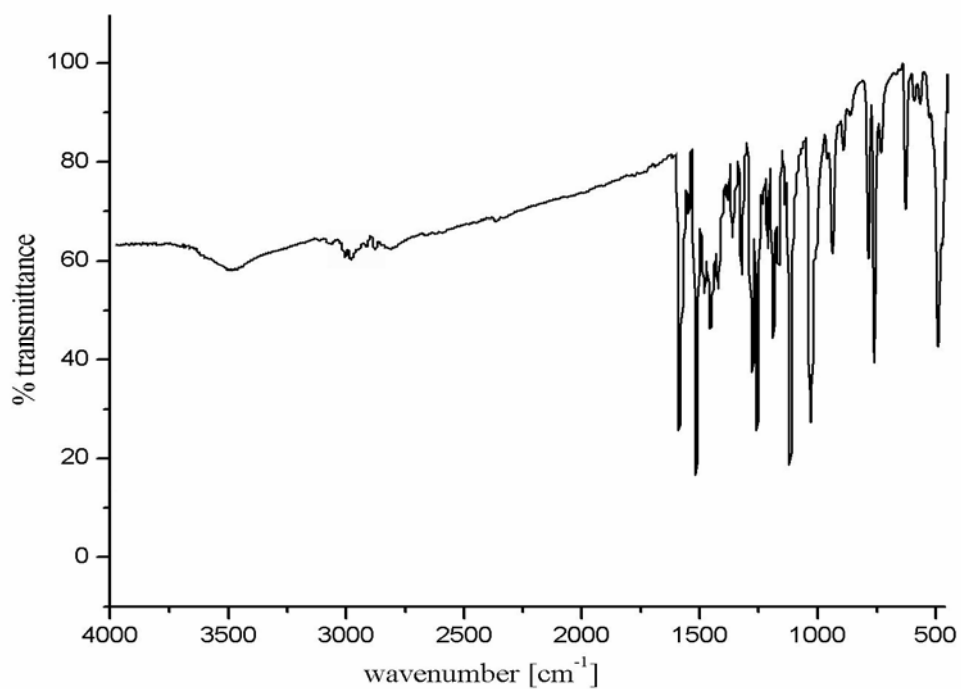**Figure 5.4:** *FTIR spectrum of the Schiff base hamp*
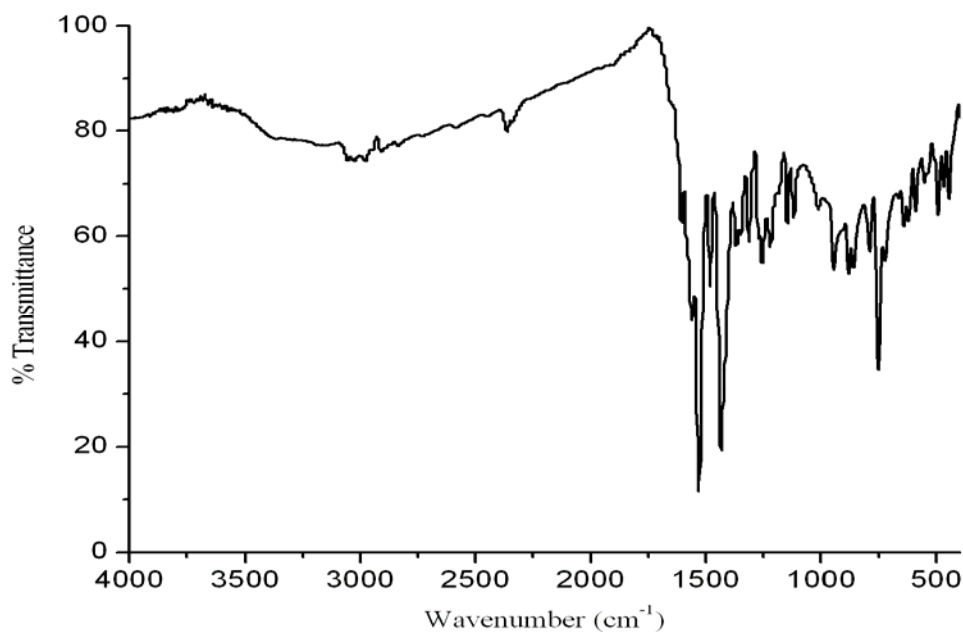
Figure 5.5: *FTIR spectrum of [Mn(hamp)(H₂O)].H₂O*

Transition metal complexes of quinoxaline based Schiff base ligands: Synthesis,
characterization and catalytic activity study

113
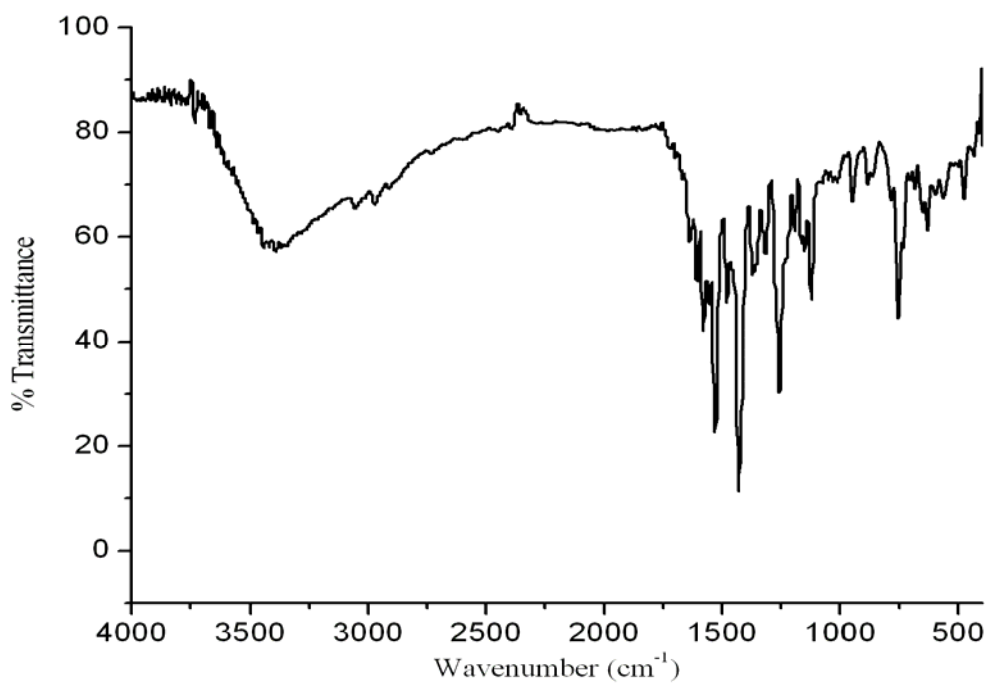
Figure 5.6: *FTIR spectrum of [Fe(hamp)Cl(H$_2$O)$_2$]*

Figure 5.7: *FTIR spectrum of [Co(hamp)(OAc)(H$_2$O)$_2$].H$_2$O*

Transition metal complexes of quinoxaline based Schiff base ligands: Synthesis, characterization and catalytic activity study
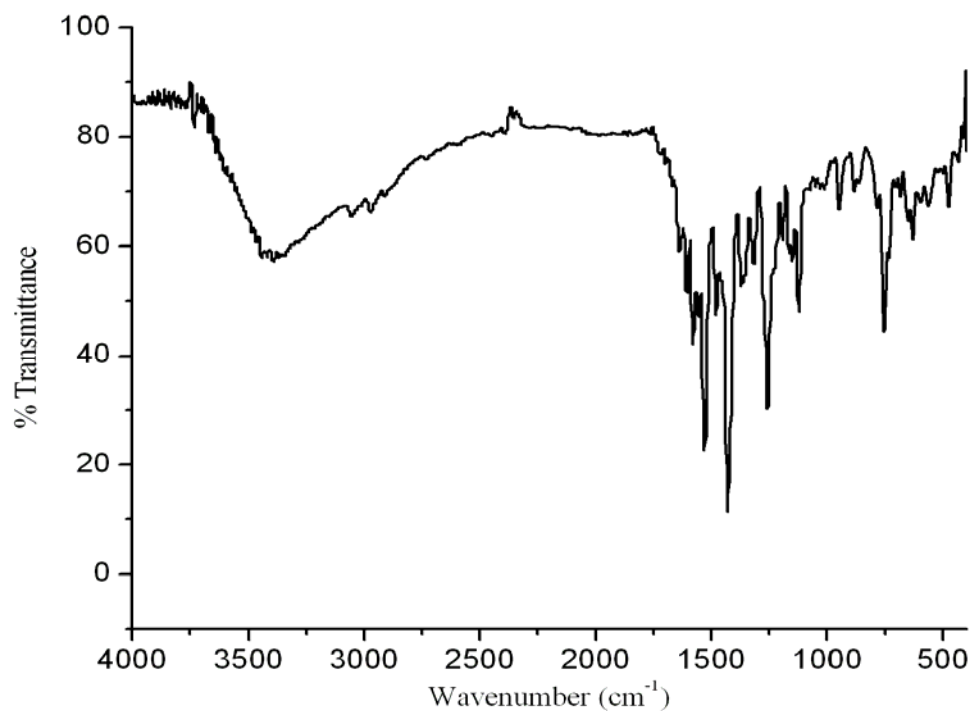
Figure 5.8: *FTIR spectrum of [Ni(hamp)(H₂O)].H₂O*
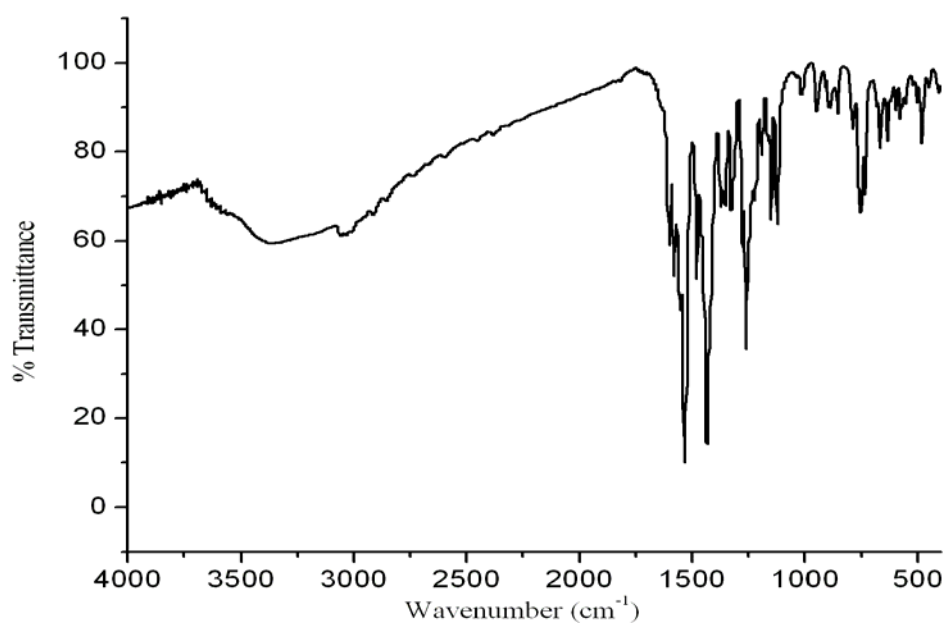
Figure 5.9: *FTIR spectrum of [Cu(hamp)(H₂O)]*

Transition metal complexes of quinoxaline based Schiff base ligands: Synthesis,
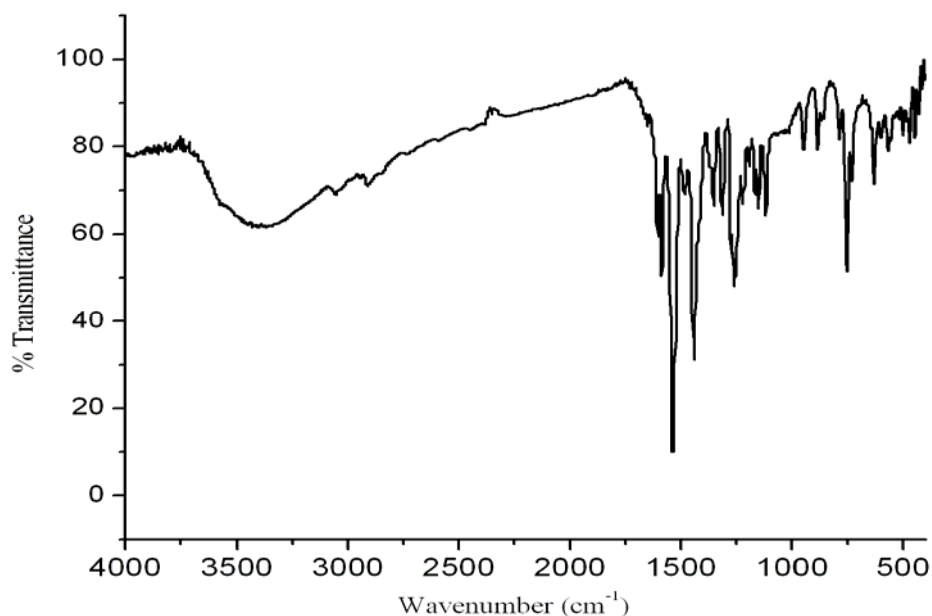characterization and catalytic activity study

115

Figure 5.10: *FTIR spectrum of [Zn(hamp)(H₂O)]*

5.3.4 Electronic spectra

The electronic spectral data of the Schiff base and complexes are presented in Table 5.5. Spectra are taken in methanol ($\sim$5x10^{-4} molar) and are given in Figures 5.11-5.17. The spectral bands due to solvent, which have been observed above 45000 cm^{-1}, are omitted [42]. The ligand shows absorptions at 30800 and 24000 cm^{-1}. These bands are attributed to benzene π–π*, imino π–π* and quinoxaline π–π* transitions of the Schiff base. In complexes, the intense bands observed above 30000 cm^{-1} are due to charge transfer and intraligand transitions.

The electronic spectrum of the manganese(II) complex in methanol contain two intense broad bands at 29800 and 21500 cm^{-1}. The weak d-d bands are masked by these charge transfer bands [43]. To get more information about geometry, the UV-Vis-NIR spectrum of the Mn(II) complex is taken in nujol mull (Figure 5.18). In the near IR region of the mull spectrum a multiplet is observed around 6200 cm^{-1}.

Such low energy bands are characteristic of tetrahedral manganese(II) compounds. The spectrum of the Fe(III) complex exhibits a weak shoulder band at 23200 cm^{-1} which may be assigned to the $^{6}A_{1g}{\rightarrow}T_{2g}(G)$ transition and indicates an octahedral geometry of the complex [43].

In the electronic spectrum of Co(II) complex the d–d transitions are almost masked by the high-intensity charge transfer bands. However, a shoulder is observed around 17000 cm^{-1} which may be assigned to the $^{4}T_{1g}(F){\rightarrow}^{4}T_{1g}(P)$ transition and transitions in this region have been reported for octahedral Co(II) complexes [32].

The solution spectrum of the nickel(II) complex shows two charge transfer bands at 29000 and 21400 cm^{-1}. The d-d bands are observed at 16100 and 11000 cm^{-1} which is due to $^{3}T_{1}{\rightarrow}^{3}T_{2}$ and $^{3}T_{1}{\rightarrow}^{3}T_{1}(P)$ transitions. The spectrum of the nickel(II) complex is also taken in nujol mull in the UV-Vis-NIR region (Figure 5.19). The near IR band characteristic of the $^{3}T_{1}(F){\rightarrow}^{3}A_{2}(F)$ transition of tetrahedral nickel(II) appears at 7100 cm^{-1} for this complex.

The copper(II) complex exhibits intense charge transfer bands at 23800 and 20400, and the band observed at 17000 cm^{-1} is due to the $^{2}T_{2}$–$^{2}E_{2}$ transition. A band is observed in the NIR region of the mull spectrum of the copper(II) complex at 6400 cm^{-1}. A band in this region has been reported for the tetrahedral copper(II) complexes (Figure 5.20) [43, 44]. The zinc(II) complex exhibits a charge transfer transition at 20300 cm^{-1}.

Transition metal complexes of quinoxaline based Schiff base ligands: Synthesis, characterization and catalytic activity study

117

Table 5.5: *The UV-Vis spectral data*

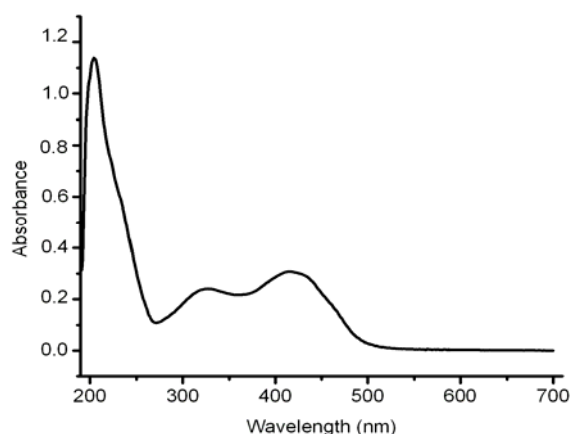| Compound	Absorption maxima (cm^{-1})	log ε (ε in L $mol^{-1}cm^{-1}$)	Assignment
hamp	30800	3.09	$\pi \rightarrow \pi^*$
	24000	3.18	$\pi \rightarrow \pi^*$
[Mn(hamp)(H₂O)]H₂O	44640	3.50	$\pi \rightarrow \pi^*$
	29800	3.11	CT
	21500	3.17	CT
[Fe(hamp)Cl(H₂O)₂]	42900	3.36	$\pi \rightarrow \pi^*$
	36400	3.27	$\pi \rightarrow \pi^*$
	29070	3.26	CT
	23200	2.66	$^6A_{1g} \rightarrow T_{2g}(G)$
[Co(hamp)(OAc)(H₂O)₂].H₂O	43510	3.64	$\pi \rightarrow \pi^*$
	29000	3.36	CT
	21400	3.42	CT
	17000	3.40	$^4T_{1g}(F) \rightarrow {}^4T_{1g}(P)$
[Ni(hamp)(H₂O)]H₂O	43200	3.68	$\pi \rightarrow \pi^*$
	30000	3.26	CT
	21300	3.39	CT
	16100	2.44	$^3T_1 \rightarrow {}^3T_2$
	11000	2.25	$^3T_1 \rightarrow {}^3T_1(P)$
[Cu(hamp)(H₂O)]	29500	3.45	$\pi \rightarrow \pi^*$
	23800	3.43	CT
	20400	3.53	CT
	17000	2.47	$^2T_2 \rightarrow {}^2E_2$
[Zn(hamp)(H₂O)]	41600	3.30	$\pi \rightarrow \pi^*$
	23800	3.33	CT
	20300	3.40	CT

Figure 5.11: *The UV-Vis spectrum of hamp*
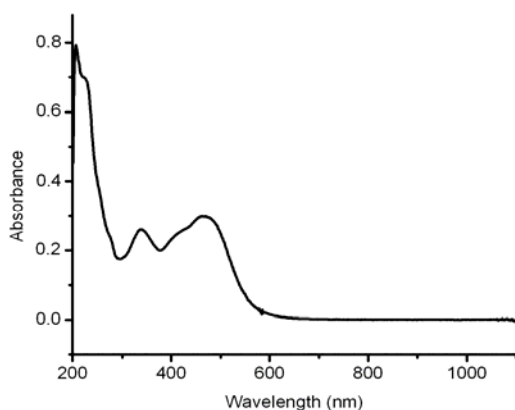
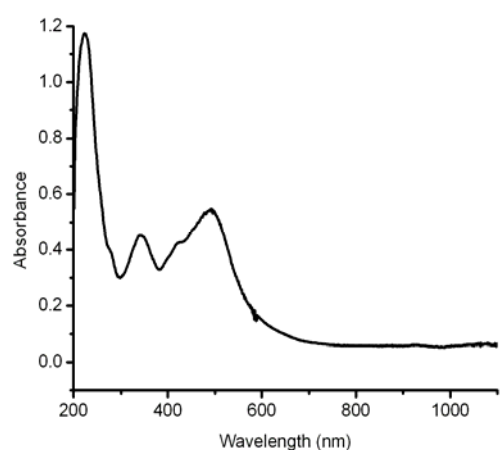**Figure 5.12:** *The UV-Vis spectrum of [Mn(hamp)(H₂O)]*
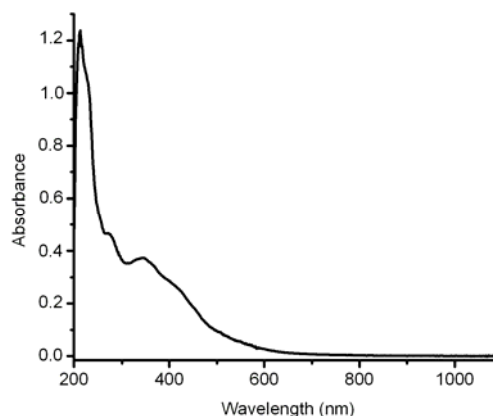
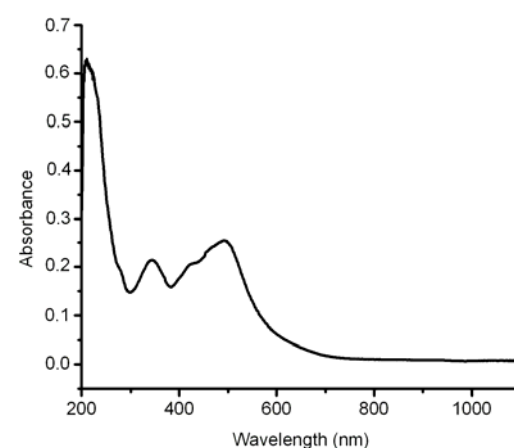**Figure 5.13:** *The UV-Vis spectrum of [Fe(hamp)Cl(H₂O)₂]*
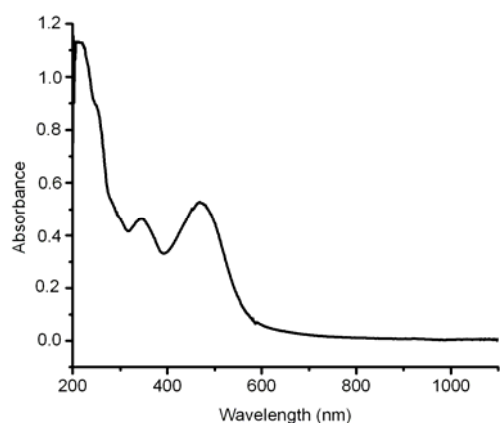
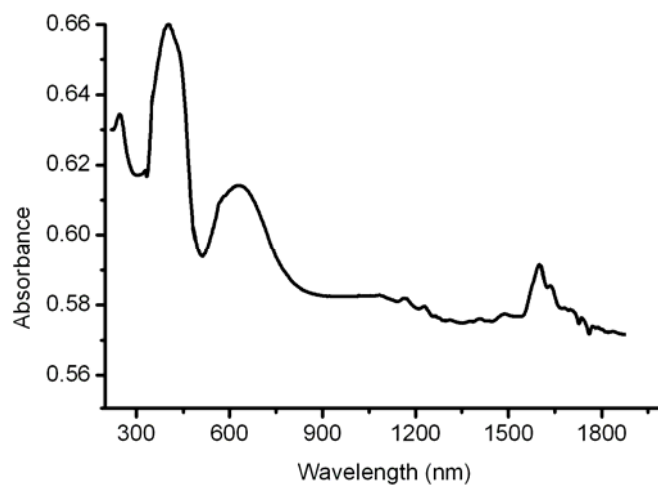**Figure 5.14:** *The UV-Vis spectrum of [Co(hamp)(OAc)]*
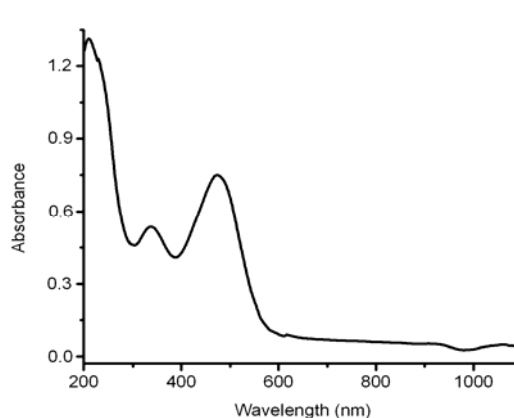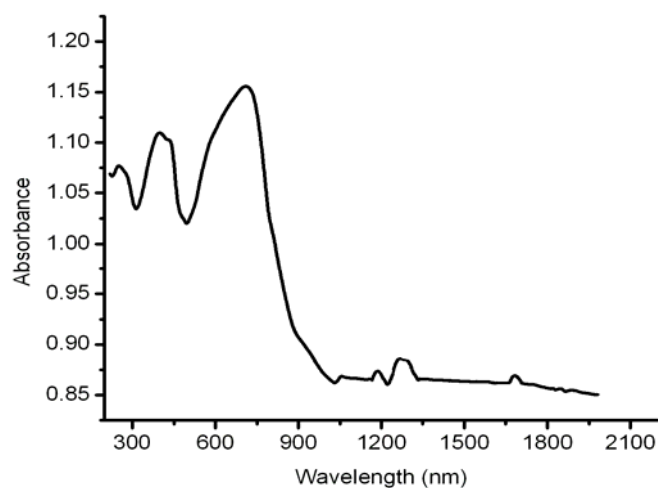
Figure 5.15: *The UV-Vis spectrum of [Ni(hamp)(H₂O)]*

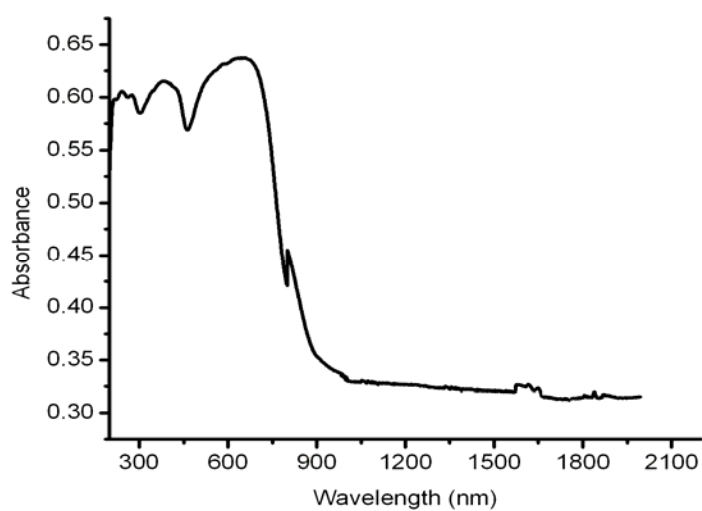**Figure 5.16:** *The UV-Vis spectrum of [Cu(hamp)(H₂O)]*

Figure 5.17: *The UV-Vis spectrum of [Zn(hamp)(H₂O)]*

Transition metal complexes of quinoxaline based Schiff base ligands: Synthesis, characterization and catalytic activity study

119

Figure 5.18: *The UV-Vis spectrum of [Mn(hamp)(H₂O)] in nujol mull*

Figure 5.19: *The UV-Vis spectrum of [Ni(hamp)(H₂O)] in nujol mull*

Figure 5.20: *The UV-Vis spectrum of [Cu(hamp)(H₂O)] in nujol mull*

5.3.5 Thermal analysis

The TG–DTG curves are presented in Figure 5.21–5.27 and the TG data in the temperature range 50-250 °C is given in Table 5.6. The ligand decomposes in two steps in the range 150–600 °C. The loss of lattice water molecule occurs in manganese(II), cobalt(II) and nickel(II) complexes below 125 °C. Loss of coordinated water in these complexes occurs in the range 130–250 °C. In the case of the Ni(II) complex, the weight loss corresponding to one lattice water and one coordinated water occurs in a continuous step from 60 to 190 °C. Above 250 °C organic part of the complexes begins to decompose. The iron(III) and copper(II) complexes show two step decomposition. Decomposition of the nickel complex takes place in three steps and the decomposition of the cobalt complex takes place in five steps.

Table 5.6: *Thermogravimetric analysis data below 200 ºC*

Complex	Temperature range, ºC	% loss	Fragment lost	Nature of water lost
[Mn(hamp)(H$_2$O)]H$_2$O	60-110	5.0	1 H$_2$O	Lattice water
	130-190	4.8	1 H$_2$O	Coordinated water
[Fe(hamp)Cl(H$_2$O)$_2$]	160-210	8.8	2 H$_2$O	Coordinated water
[Co(hamp)(OAc)(H$_2$O)$_2$]H$_2$O	50-110	3.9	1 H$_2$O	Lattice water
	150-210	8.4	2 H$_2$O	Coordinated water
[Ni(hamp)(H$_2$O)]H$_2$O	60-190	9.7	2 H$_2$O	Lattice water Coordinated water
[Cu(hamp)(H$_2$O)]	140-195	5.2	1 H$_2$O	Coordinated water
[Zn(hamp)(H$_2$O)]	140-180	4.6	1 H$_2$O	Coordinated water
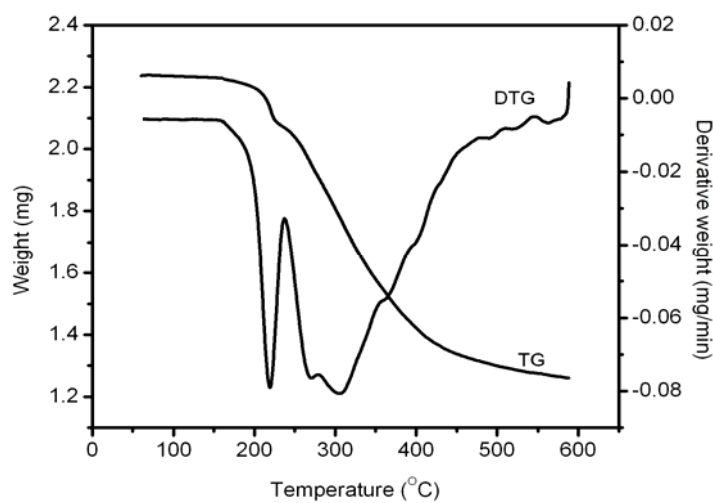
Figure 5.21: *TG-DTG of hamp*

Figure 5.22: *TG-DTG of [Mn(hamp)(H₂O)]H₂O*
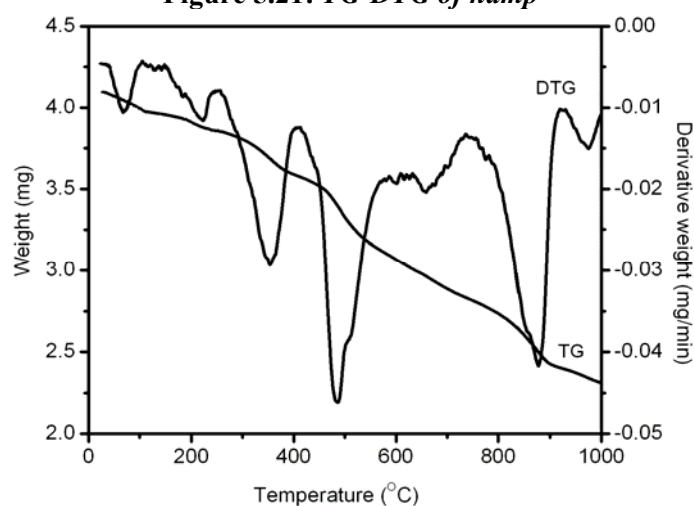
Figure 5.22: *TG-DTG of $[Mn(hamp)(H_2O)]H_2O$*
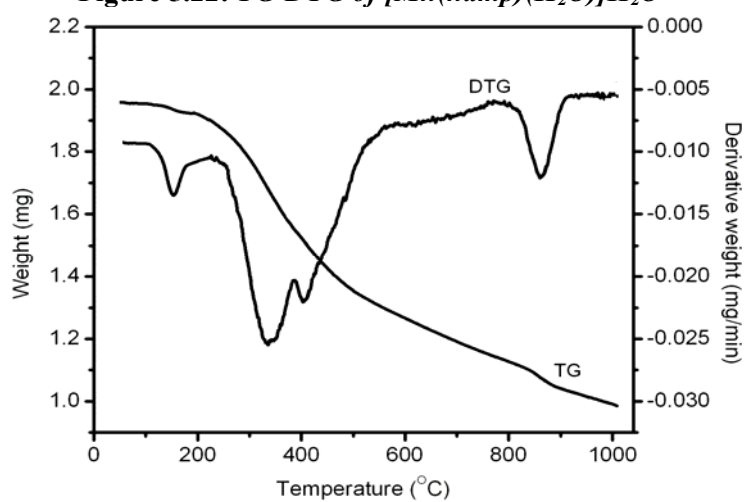
Figure 5.23: *TG-DTG of $[Fe(hamp)Cl(H_2O)_2]$*

Transition metal complexes of quinoxaline based Schiff base ligands: Synthesis, characterization and catalytic activity study
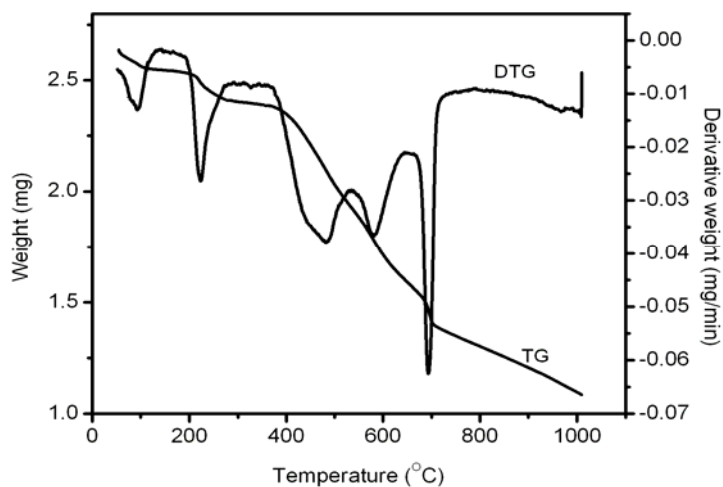
Figure 5.24: *TG-DTG of [Co(hamp)(OAc)(H₂O)₂]H₂O*
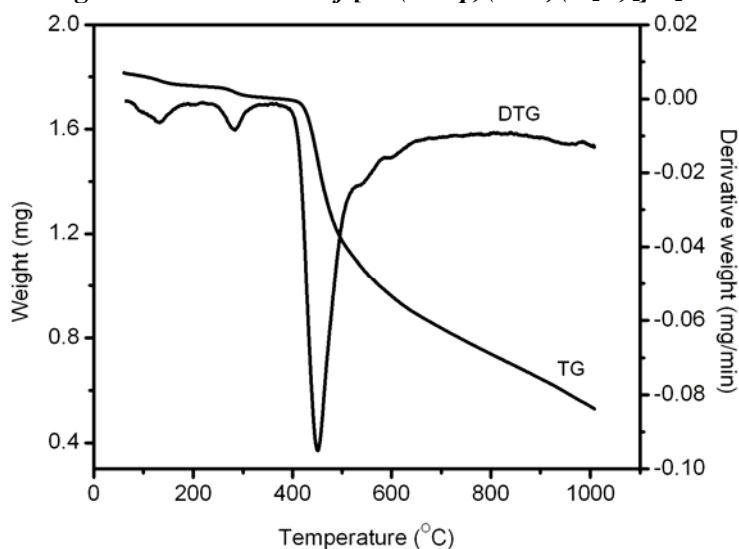
Figure 5.25: *TG-DTG of [Ni(hamp)(H₂O)]H₂O*
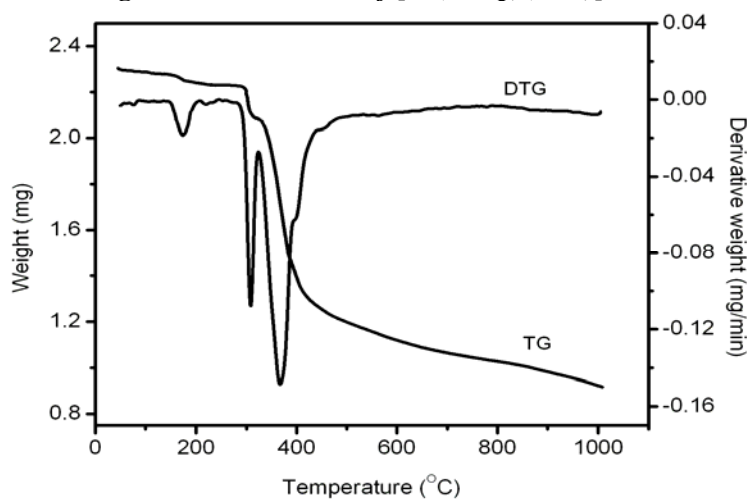
Figure 5.26: *TG-DTG of [Cu(hamp)(H₂O)]*

Transition metal complexes of quinoxaline based Schiff base ligands: Synthesis,
characterization and catalytic activity study
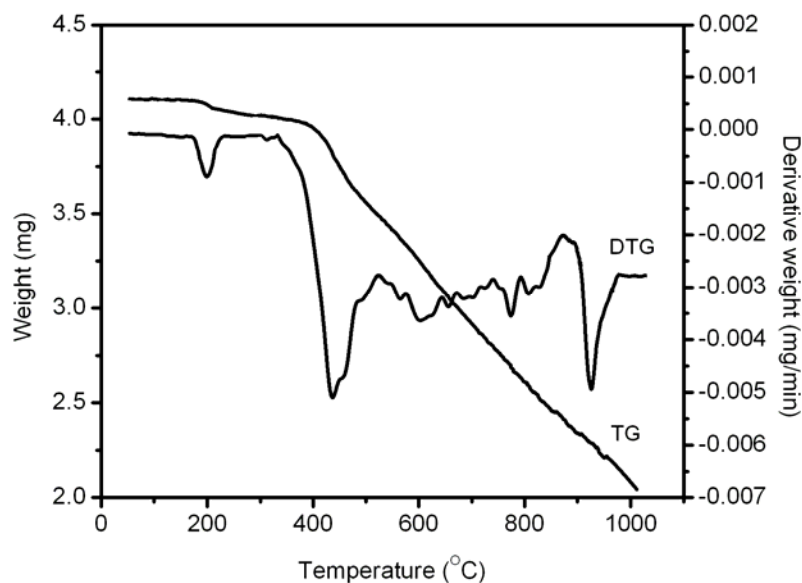
123

Figure 5.27: *TG-DTG of [Zn(hamp)(H₂O)]*

5.3.6 EPR spectra

In polycrystalline state, manganese(II) complex gives a broad signal with a *g* value of 2.06 [45]. The spectrum at 77 K in DMSO (Figure 5.28) exhibits six hyperfine lines. The lines are poorly resolved, which may be due to the poor glass formation. The spectrum gives a *g* value of 1.99 with an A value of 0.00929 cm^{-1}.

In polycrystalline state EPR spectrum of the copper(II) complex gives an isotropic spectrum with a *g* value of 1.99 (Figure 5.29). This may be due to the extensive exchange coupling through misalignment of the local molecular axes between different molecules in the unit cell (dipolar broadening) and enhanced spin lattice relaxation. Solution state EPR spectrum of the copper complex was recorded in DMF at 77K. The $g_{\parallel}$ value is found to be 2.08 and $g\perp$ is 1.99. The spectrum clearly indicates axial features [46].
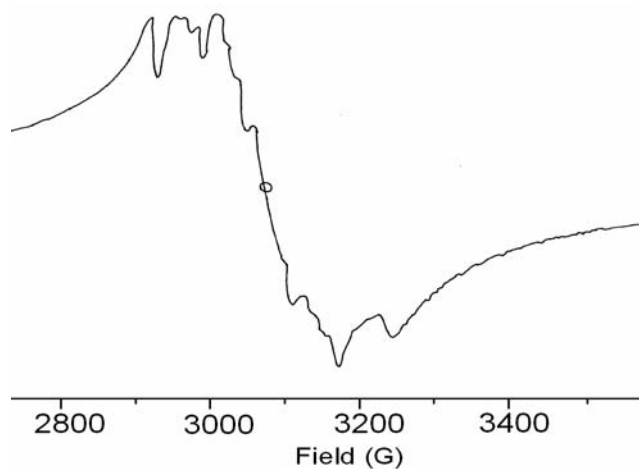
Figure 5.28: *EPR spectrum of [Mn(hamp)(H₂O)]H₂O in DMSO, 77 K*
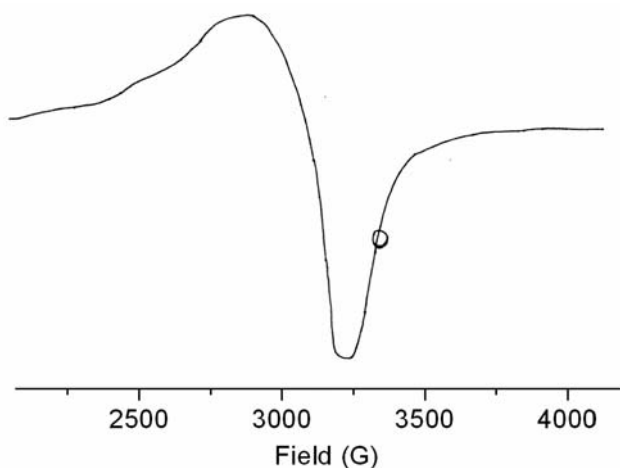
Figure 5.29: *EPR spectrum of [Cu(hamp)(H₂O)] in polycrystalline state*

5.4 CONCLUSIONS

A new Schiff base derived from 3-hydroxy quinoxaline-2-carboxaldehyde and 2-amino-5-methylphenol and its complexes of Mn(II), Fe(III), Co(II), Ni(II), Cu(II) and Zn(II) have been synthesized and characterized. Based on the physicochemical and spectroscopic studies we propose the following structures for the complexes (Figure 5.30).

Transition metal complexes of quinoxaline based Schiff base ligands: Synthesis,
characterization and catalytic activity study

125
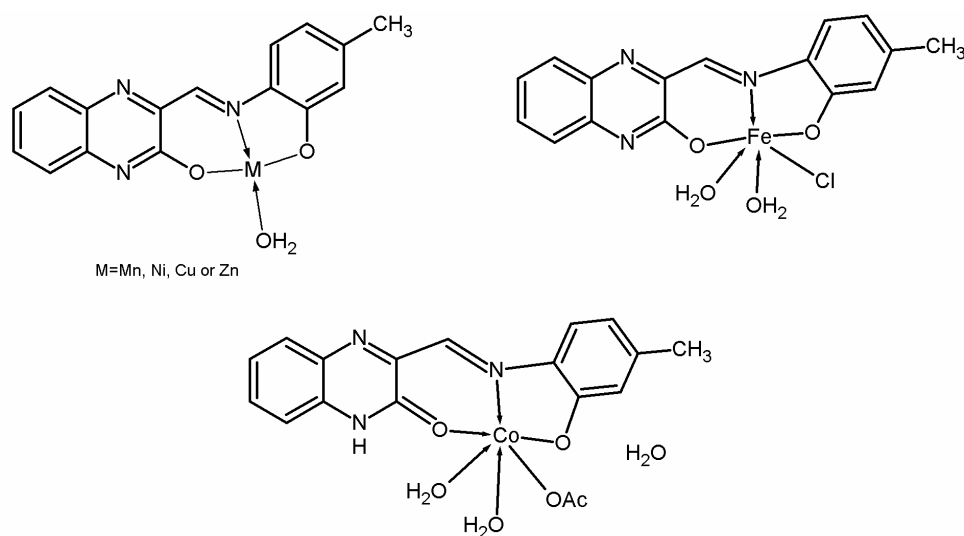
Figure 5.30: *The proposed geometry of complexes*

References

1.   M.R. Maurya, H. Saklani, A. Kumar, S. Chand, *Cat. Lett.* 93 (2004) 121.

2.   A.A.A. Emara, O.M.I. Adly, *Transition Met. Chem.* 32 (2007) 889.

3.   K.C. Gupta, A.K. Sutar, *Coord. Chem. Rev.* 252 (2008) 1420.

4.   R.M. Mahfouz, *Isotopes in Environmental and Health Studies* 26 (1990) 68.

5.   A. Kagkelari, G.S. Papaefstathiou, C.P. Raptopoulou, T.F. Zafiropoulos, *Polyhedron* 28 (2009) 3279.

6.   P.S.Chittilappilly, K.K.M.Yusuff, *Indian J. Chem.. Sect. A* 47 (2008) 848.

7.   G. Das, R. Shukla, S. Mandal, R. Singh, P.K. Bharadwaj, *Inorg. Chem.* 36 (1997) 323.

8.   M. Valko, R. Klement, P. Pelikan, R. Boca, R. Dlhan, A. Böttcher, H. Elias, L. Müller, *J. Phys. Chem.* 99 (1995) 137.

9.   E. Keskioğlu, A. B. Gündüzalp, S. Cete, F. Hamurcu, B. Erk, *Spectrochim. Acta A* 70 (2008) 634.

10.   R.N. Patel, N. Singh, V.L.N. Gundla, *Polyhedron* 25 (2006) 3312.

11.   R.N. Patel, V.L.N. Gundla, D.K. Patel, *Polyhedron* 27 (2008) 1054.

12. I.I. Mathews, P. Ajoy, S. Vasudevan, and H. Monahar, *Inorg. Chem*. 30 (1991) 2181.

13. K.S. Bai, D.L. Leussing, *J. Am. Chem. Soc*. 89 (1967) 6126.

14. H. Demirelli, F. Köseoğlu, *J. Sol. Chem*. 34 (2005) 561.

15. K. Severin, R. Bergs, W. Beck, *Angew. Chem. Int.* 37 (1998) 1634.

16. D. J. Brown, *The chemistry of heterocyclic compounds, Quinoxalines supplement 2*, John Wiley & Sons, Inc., Hoboken, New Jersey (2004).

17. Y-J. Seok, K-S. Yang, S-T. Kim, W-K. Huh, S-O. Kang, *J. Carbohydr. Chem*. 15 (1996) 1085.

18. A.P. Kulkarni, Y. Zhu, S.A. Jenekhe, *Macromolecules* 38 (2005) 1553.

19. M.S. De Groot, I.A.M. Hesselmann, J. Schmidt, J.H. Van Der Waals, *Mol. Phys*. 100 (2002) 31.

20. E.R. Kotb, M.A. Anwar, M.S. Soliman, M.A. Salama, *Phosphorus, Sulfur Silicon Relat. Elem.* 182 (2007) 1119.

21. X-H. Bu, H. Liu, M. Du, K.M-C. Wong, V.W-W. Yam, *Inorg. Chim. Acta* 333 (2002) 32.

22. S. Mayadevi, K.K.M. Yusuff, *Synth. React. Inorg. Met.-Org. Chem*. 27 (1997) 319.

23. W.J. Geary, *Coord. Chem. Rev*. 7 (1971) 81.

24. M. Asadi, K. Mohammadi, S. Esmaielzadeh, B. Etemadi, H.K. Fun, *Polyhedron* 28 (2009) 1409.

25. M. Kabak, A. Elmali, Y. Elerman, *J. Mol. Str.* 470 (1998) 295.

26. K. S. Abou-Melha, *J. Coord. Chem.* 61 (2008) 2053.

27. H. Ünver, K. Polat, M. Uçar, D. M. Zengin, *Spectrosc. Lett.* 36 (2003) 287.

28. N.A. Öztaş, G. Yenişehirli, N. Ancın, S.G. Öztaş¸ Y. Özcan, S. İde, *Spectrochim. Acta A* 72 (2009) 929.

29. M. Shebl, *Spectrochim. Acta A* 73 (2009) 313.

Transition metal complexes of quinoxaline based Schiff base ligands: Synthesis, characterization and catalytic activity study

127

30. W.F. Zeng, Y.H. Chen, M.Y. Chiang, C.P. Cheng, *Polyhedron* 26 (2007) 1303

31. Rob Janes, Elaine A. Moore, *Metal-ligand bonding*, Page 39, Royal Society of Chemistry, Cambridge, UK

32. F.A. Cotton, G. Wilkinson, C.A. Murillo, M. Bochmann, *Advanced Inorganic Chemistry*, sixth edn., Wiley, New York (1999).

33. P.K. Samal, A.K. Patra, M. Nethaji, A.R. Chakravarthy, *Inorg. Chem.* 46 (2007) 11112.

34. P. Mayer a, K.C. Potgieter b, T.I.A. Gerber, *Polyhedron* 29 (2010) 1423.

35 A. Khandar, B. Shaabani, F. Belaj, A. Bakhtiari, *Polyhedron* 25 (2006) 1893.

36 S.M.E. Khalil, A.A.A. Emara, *J. Coord. Chem.* 55 (2002) 17.

37 D. Gegiou, E. Lambi, E. Hadjoudis, *J. Phys. Chem.* 100 (1996) 17762.

38 K. Nakamoto, *Infrared and Raman Spectra of Inorganic and Coordination Compounds*, 4th ed., John Wiely and Sons, Inc, New York (1986).

39 M. Patel, M.M. Patel, A. Ray, M.R. Patel, *J. Inorg. Nucl. Chem.* 43 (1980) 509.

40 S. Mayadevi, G.P. Preetha, K.K.M. Yusuff, *Synth. React. Inorg. Met.-Org. Chem.* 33 (2003) 481.

41 S.M. Abdallah, G.G. Mohamed, M.A. Zayed, M.S. Abou El-Ela, *Spectrochim. Acta A* 73 (2009) 833.

42 D.L. Pavia, G.M. Lampman, G.S. Kriz, J.A. Vyvyan, *Introduction to spectroscopy*, 4th edition, Brooks Cole (2009).

43 A.B.P. Lever, *Inorganic Electronic Spectroscopy*, 2nd Edn, Elsevier, Amsterdam (1984).

44 R. longhi, R.S. Drago, *Inorg. Chem.* 4 (1964) 11.

45 A. Sreekanth, M. Joseph, H-K. Fun, M.R.P. Kurup, *Polyhedron* 25 (2006) 1408.

46 U.L. Kala, S. Suma, M.R.P. Kurup, S. Krishnan, R.P. John, *Polyhedron* 26 (2007) 1427.

........ॐ......